AD NUMBER
AD638208
LIMITATION CHANGES
TO: **Approved for public release; distribution is unlimited.**
FROM: **Distribution: Further dissemination only as directed by Bureau of Shipd (Navy), Washington, DC, 01 FEB 1961, or higher DoD authority.**
AUTHORITY
BUSHIPS per DTIC form 55

THE FLOW FIELD OF AN INFINITELY BLADED PROPELLER WITH RADIALLY NON-UNIFORM LOADING

by

Bohyun Yim and C. F. Chen

February 1, 1961

TECHNICAL REPORT 005-2

THE FLOW FIELD OF AN INFINITELY BLADED PROPELLER WITH RADIALLY NON-UNIFORM LOADING

by

Bohyun Yim and C. F. Chen

February 1, 1961

Prepared Under

Bureau of Ships
Department of the Navy
Contract No. NObs-78451

TABLE OF CONTENTS

LIST OF FIGURES

LIST OF SYMBOLS

A	a field point where the induced flow field of the propeller is to be evaluated (see Figure 1)
A_1	a source point on the propeller disk (see Figure 1)
B	complete elliptic integral as defined by equation [17]
C	constant defined by equation [7]
C_T	thrust coefficient $= \dfrac{T}{\frac{1}{2}\rho V^2 S_p}$
k	argument of complete elliptic integral defined by equation [15]
k_1	argument of complete elliptic integral defined by equation [19]
K	complete elliptic integral of the first kind
n	power index of the assumed loading variation, equation [5]
p	perturbed pressure, i.e., pressure at any point minus the pressure in the uniform stream
Δp	pressure jump across the propeller disk
P	Legendre function
r	radial coordinate
r_o	$= \sqrt{x^2 + r^2}$ (see Figure 1)
R	propeller radius
S_p	propeller disk area
v_r	perturbation velocity in the radial direction
v_x, v_y, v_z	perturbation velocity in the x-, y-, and z- direction
V	uniform stream velocity
x, y, z	cartesian coordinates
θ	angular coordinate of the field point
θ_1	angular coordinate of the source point

θ_o	$\cos^{-1}(\frac{x}{r_o})$ (see Figure 1)
ρ	density of fluid
Φ	velocity potential exterior to the propeller slipstream
ω	distance between the source point A_1 and field point A (see Figure 1)

Prime denotes differentiation with respect to the argument.

ABSTRACT

The flow field of an infinitely bladed propeller of disk loading proportional to $(r/R)^n \cdot (1-r/R)$ in an incompressible, inviscid fluid is expressed in terms of a series of Legendre functions. Numerical calculations have been carried out for the case $n = 5$. The radial velocity at $r = R$, and the shape of the stream surface passing through the periphery of the propeller disk are determined and compared to that of uniform disk loading.

THE FLOW FIELD OF AN INFINITELY BLADED PROPELLER WITH RADIALLY NON-UNIFORM LOADING

I. Introduction.

The marine propulsion system consisting of a propeller enclosed by a nozzle has found many useful applications, especially when high disk loadings are required. Since the advent of the supercavitating propellers, it has been suggested by Tulin that a nozzle-supercavitating propeller system can extend to lower speeds the range of speeds in which a supercavitating propeller can be practically operated. In order to make a rational design of such a system, and to predict performance both at design and other forward speeds, a knowledge of the flow field, especially of the radial component of velocity near the tip of the propeller, is needed.

The flow field of an infinitely bladed propeller in an incompressible, inviscid fluid may be calculated using either one of the following two equivalent methods: (1) by solving the exact continuity equation together with boundary condition at the propeller disk derived from the linearized Bernoulli's equation, or (2) by solving the Laplace equation for the perturbed pressure p derived from the linearized equation of motion, together with the specified pressure jump across the propeller disk. With both of these methods, the propeller is considered to be lightly loaded, otherwise the equations concerned cannot be linearized. The problem then reduces to the solution of the Laplace equation with specified boundary conditions; solutions may be obtained either by separation of variables or through a suitable distribution of singularities. For propellers with uniform loading, the solution has been given by Küchemann and Weber (1953), Meyerhoff and Finkelstein (1958) and others. Tachmindji (1959) has given the axial

velocity field of a propeller with optimum (non-uniform) loading.

In the solution of the uniformly loaded disk (cf. Küchemann and Weber, 1953), the radial component of the induced velocity exhibits a logarithmic singularity at the periphery of the propeller disk. Since logarithmic singularities are integrable, the streamline near the propeller tip is continuous but with infinite slope. The region influenced by this singular radial velocity is very small compared to the radius (less than 0.0001 R), but nevertheless troublesome. In the belief that this singular behavior arises out of the discontinuous loading at the periphery, it was decided to investigate loadings which decrease to zero continuously at the periphery of the propeller disk.

In this report, starting with the Laplace equation governing the perturbation pressure p, we obtain the solution to the problem in which the propeller loading varies as $(r/R)^n(1-r/R)$, where R is the radius of the propeller, in terms of a series of Legendre functions. Numerical calculations have been carried out for the case $n = 5$. Values for the radial component of the perturbation velocity at $r = R$ are determined and are compared with those obtained for the case of uniform loading. The shape of the streamline passing through the propeller tip has also been determined and compared with the case of uniform loading. Although the radial components of the perturbation velocities very close to the propeller tip for these two loadings are quite different in character, the resulting streamline shapes are on the whole quite similar.

II. Velocity Field.

The linearized equations of motion for the perturbed physical variables, pressure and velocity, in rectangular coordinates as shown in Figure 1 are:

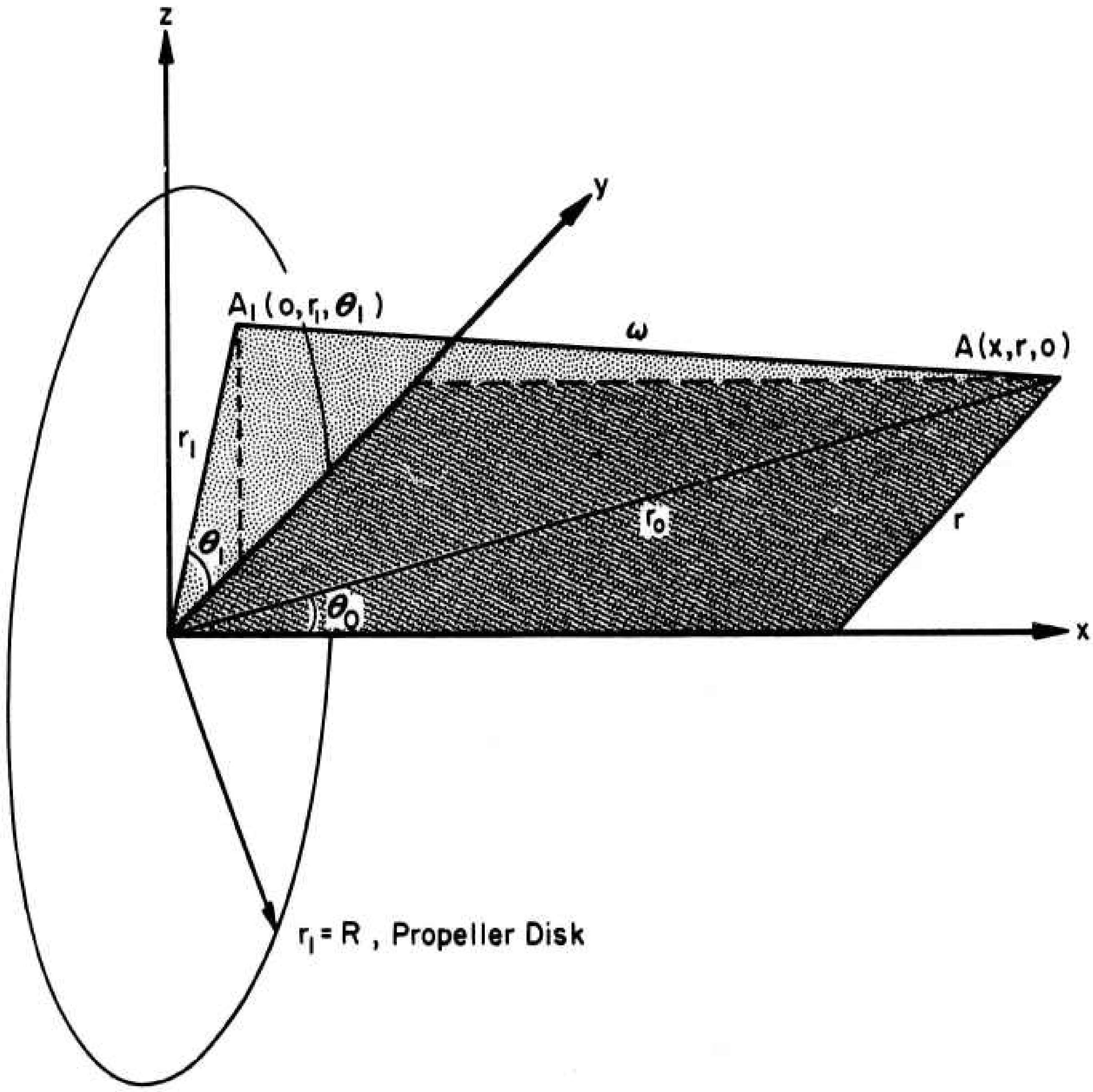

Figure 1 – Coordinate System

$$\rho V \frac{\partial v_x}{\partial x} = - \frac{\partial p}{\partial x} + X$$

$$\rho V \frac{\partial v_y}{\partial x} = - \frac{\partial p}{\partial y} \qquad [1]$$

$$\rho V \frac{\partial v_z}{\partial x} = - \frac{\partial p}{\partial z}$$

$$\frac{\partial v_x}{\partial x} + \frac{\partial v_y}{\partial y} + \frac{\partial v_z}{\partial z} = 0 \qquad [2]$$

where X is the force per unit volume which is imparted to the fluid by the propeller disk, V is the velocity of the uniform stream, and v_x, v_y, and v_z are perturbed velocity components. From these equations, one easily obtains the Laplace equation for the pressure (except at the propeller disk where a jump in pressure occurs):

$$\nabla^2 p = 0. \qquad [3]$$

In axisymmetric flow, as in the present case, equation [3] may be written in the cylindrical coordinate system as

$$\frac{1}{r} \frac{\partial}{\partial r} \left(r \frac{\partial p}{\partial r}\right) + \frac{\partial^2 p}{\partial x^2} = 0, \qquad [4]$$

where x and r are the axial and radial coordinates respectively. The specified pressure jump at the propeller disk, i.e., for x = 0 and $r \leq R$, is taken for the loadings under consideration as:

$$\frac{\Delta p}{\frac{1}{2}\rho V^2} = \frac{(n+2)(n+3)}{2} \; C_T \left(\frac{r}{R}\right)^n \left(1 - \frac{r}{R}\right), \qquad [5]$$

in which C_T is the thrust coefficient of the propeller. The solution to equation [4] satisfying the boundary condition [5] can be obtained by a distribution of doublets, with strength equal to

the pressure jump, at the propeller disk. We shall use subscript 1 to denote the source point A_1 ($x_1 = 0$, r_1, θ_1) on the propeller disk. Because of axisymmetry, we consider the field point A (x,r,0) to be in the xy plane, as shown in Figure 1. The distance between A and A_1 is indicated by ω. For the sake of convenience, we consider all distances are non-dimensionalized with respect to the radius of the propeller R in the mathematical treatment. But the numerical results, as presented in plots, are presented in the actual physical coordinate system.

The pressure p is given by

$$p(x,r) = \frac{C}{4\pi}\int_{S_p} r_1^n \,(1-r_1)\, \frac{\partial}{\partial x_1}\left(\frac{1}{\omega}\right) dS, \qquad [6]$$

where

$$C = \tfrac{1}{2}\rho V^2 C_T \,\frac{(n+2)(n+3)}{2}, \qquad [7]$$

and S_p denotes the surface area of the propeller disk. Equation [6] may be written as

$$p(x,r) = \frac{C}{4\pi}\frac{\partial}{\partial x_1}\int_0^1 r_1^{\,n+1}\,(1-r_1)dr_1 \int_0^{2\pi} \frac{\partial\theta_1}{\omega} \qquad [8]$$

The θ_1 integral in [8] may be written in terms of Legendre functions, as shown by Kellogg (1953),

$$\int_0^{2\pi} \frac{d\theta_1}{\omega} = \frac{2\pi}{r_o}\left[1-\tfrac{1}{2}\left(\frac{r_1}{r_o}\right)^2 P_2(\cos\theta_o) + \frac{1\cdot 3}{2\cdot 4}\left(\frac{r_1}{r_o}\right)^4 P_4(\cos\theta_o) - \frac{1\cdot 3\cdot 5}{2\cdot 4\cdot 6}\left(\frac{r_1}{r_o}\right)^6 P_6(\cos\theta_o) + \dots\right], \text{ for } r_o > r_1, \qquad [9]$$

where $r_o^2 = r^2 + x^2$, and $\cos\theta_o = \frac{x}{r_o}$, see Figure 1. Hence at any point such that $r_o > 1$, we have

$$p(x,r) = \frac{C}{2}\frac{\partial}{\partial x_1}\left[\frac{1}{r_o}\left\{\frac{1}{(n+2)(n+3)} - \frac{1}{2(n+4)(n+5)}\left(\frac{1}{r_o}\right)^2 P_2(\cos\theta_o)\right.\right.$$
$$\left.\left. + \frac{1\cdot 3}{2\cdot 4(n+6)(n+7)}\left(\frac{1}{r_o}\right)^4 P_4(\cos\theta_o) + \ldots\right\}\right] . \qquad [10]$$

From the first equation of [1], we obtain for points outside the slipstream

$$v_x = -\frac{p}{\rho V} . \qquad [11]$$

Outside the slipstream, there exists a velocity potential Φ which may be obtained as

$$\Phi = -\int_{-\infty}^{x} v_x dx. \qquad [12]$$

Noting the relations

$$\left\{\begin{aligned} \frac{\partial r_o}{\partial x_1} &= -\frac{\partial r_o}{\partial x} \\ \frac{\partial \cos\theta_o}{\partial x_1} &= -\frac{\partial \cos\theta_o}{\partial x} , \end{aligned}\right. \qquad [13]$$

we obtain from equation [12]

$$\Phi = \int_{-\infty}^{x} \frac{p}{\rho V} dx$$

$$\Phi = -\frac{C}{2\rho V r_o}\left[\frac{1}{(n+2)(n+3)} - \frac{1}{2(n+4)(n+5)}\left(\frac{1}{r_o}\right)^2 P_2(\cos\theta_o) + \frac{1\cdot 3}{2\cdot 4\cdot(n+6)(n+7)}\left(\frac{1}{r_o}\right)^4 \cdot P_4(\cos\theta_o) + \ldots\right],$$

$$\text{for } x > 0,\ r_o > 1. \qquad [14]$$

This result is exactly the same as that of Korvin-Kroukovsky(1956) for the special case of uniform loading. Now,

$$v_r(x,r) = -\frac{\partial\Phi}{\partial r}$$

$$= -\frac{C_T V}{8}(n+2)(n+3)\left\{\frac{r}{r_o^3}\left[\frac{1}{(n+2)(n+3)} - \frac{1\cdot 3}{2(n+4)(n+5)}\left(\frac{1}{r_o}\right)^2 P_2(\cos\theta_o) + \frac{1\cdot 3\cdot 5}{2\cdot 4\cdot(n+6)(n+7)}\left(\frac{1}{r_o}\right)^4 P_4(\cos\theta_o) + \ldots\right]\right.$$

$$\left. + \frac{xr}{r_o^4}\left[\frac{1}{2(n+4)(n+5)}\left(\frac{1}{r_o}\right)^2 P_2'(\cos\theta_o) - \frac{1\cdot 3}{2\cdot 4\cdot(n+6)(n+7)}\left(\frac{1}{r_o}\right)^4 P_4'(\cos\theta_o) + \ldots\right]\right\} \text{ for } r_o > 1, \qquad [15]$$

where the prime denotes differentiation with respect to the argument. Equation [11], together with [10], give the axial component, and equation [15] gives the radial component of the perturbed velocity outside a sphere of radius 1 due to a propeller with loading given by equation [5]. The axial component, $(v_x - v_x\big|_{x=0})$, is antisymmetric and the radial component, v_r, is symmetric with respect to the plane x = 0.

We shall now let $n = 5$ in the loading expression [5]. The resulting pressure jump along a radius of the propeller disk is given in Figure 2. This distribution is chosen for the following reasons: (1) the occurrence of the maximum loading near the tip, $r/R = 0.833$, may closely approximate the loadings on certain propellers enclosed by a nozzle, and (2) the near zero loading near the center may approximate the presence of a hub. For this loading then, the radial component of the perturbed velocity at $r = 1$ is

$$\frac{v_r(x,1)}{C_T V} = -\frac{1}{8r_o^3} + \frac{7}{r_o^3}\sum_{m=1}^{\infty}\left\{\frac{P_{2m}(0)}{(7+2_m)(8+2_m)}\left(\frac{1}{r_o}\right)^{2m} \cdot \left[(-1)^{m+1}(2m+1)P_{2m}(\cos\theta_o)-(-1)^m\frac{1}{2m}P'_{2m}(\cos\theta_o)\right]\right\}. \quad [16]$$

For $x > 0.4$, this series converges quite rapidly, terms up to and including $P_{10}(\cos\theta_o)$ are used to evaluate $v_r(x,1)$. At $x = 0$, the Legendre functions are expressible in terms of gamma functions of integer argument, which, for large values of m, may be approximated by Stirling's formula. Using the integral method of summing up the monotonically decreasing terms for large m, the value of $v_r(0,1)$ is obtained with a maximum error of 3 percent. For $0 < x \leq 0.4$, because convergence of the series is quite slow, terms up to and including $P_{16}(\cos\theta_o)$, as tabulated by Tallqvist (1937), are used in the summation. Error estimates are very difficult to make. In order to check the results thus obtained, we resort to a direct numerical integration of equation [8].

First, according to Kellogg (1953), the θ_1 integral in [8] is evaluated as

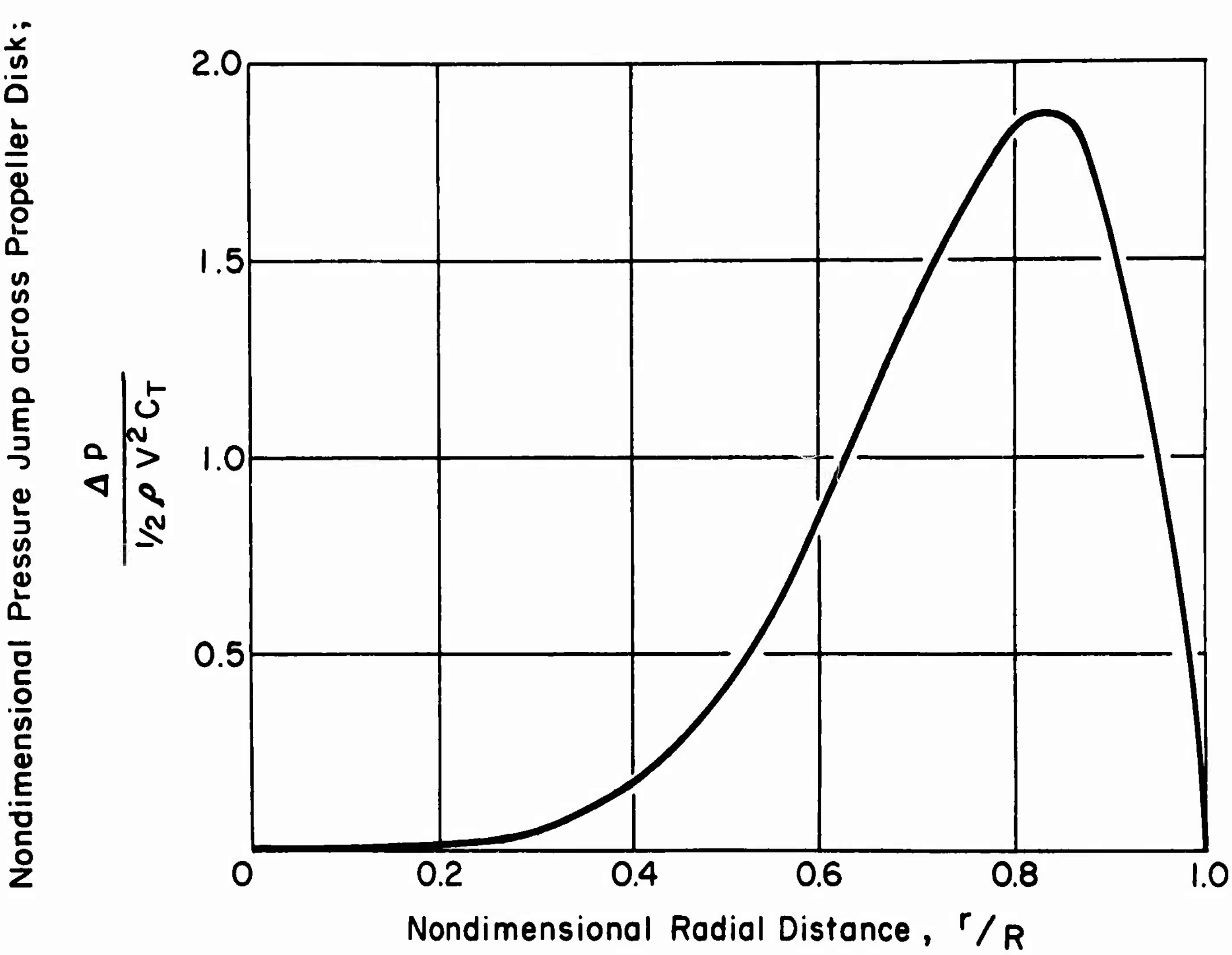

Figure 2 – Assumed Pressure Jump Variation along the Radius of the Propeller

$$\int_0^{2\pi} \frac{d\theta_1}{\omega} = \int_0^{2\pi} \frac{d\theta_1}{\sqrt{r^2+x^2+r_1^2 - 2r_1 r\cos\theta_1}} = \frac{4K(k)}{\sqrt{(r+r_1)^2+x^2}} , \qquad [17]$$

in which K is the complete elliptic integral of the first kind, and

$$k^2 = 1- \frac{(r-r_1)^2+ x^2}{\sqrt{(r+r_1)^2+ x^2}} . \qquad [18]$$

By the same process as before, we obtain

$$\frac{v_r(x,1)}{C_T V} = - \frac{14}{\pi} \int_0^1 \frac{r_1^6(1-r_1)dr_1}{\left[(1+r_1^2)+x^2\right]^{3/2}} \left\{ (1+r_1)\ K(k) \right.$$

$$\left. + B(k) \left[(1-r_1) \frac{(1+r_1)^2+x^2}{(1-r_1)^2+x^2} - (1+r_1) \right] \right\}, \qquad [19]$$

where B(k), as defined in Jahnke and Emde (1945), is

$$B(k) = \int_0^{\pi/2} \frac{\cos^2\phi\, d\phi}{\sqrt{1-k^2\sin\phi}} . \qquad [20]$$

The integral in equation [19] is evaluated numerically using Simpson's rule for points $0 < x \leq 0.4$. The results of $v_r(x,1)/C_T V$ are within 10 percent of those obtained by summing the series. The values of $v_r(x,1)$ are plotted in Figure 3.

The flow field of a uniformly loaded propeller has been given by Küchemann and Weber (1953). In particular, downstream of the propeller $v_r(x,1)$ is expressed as

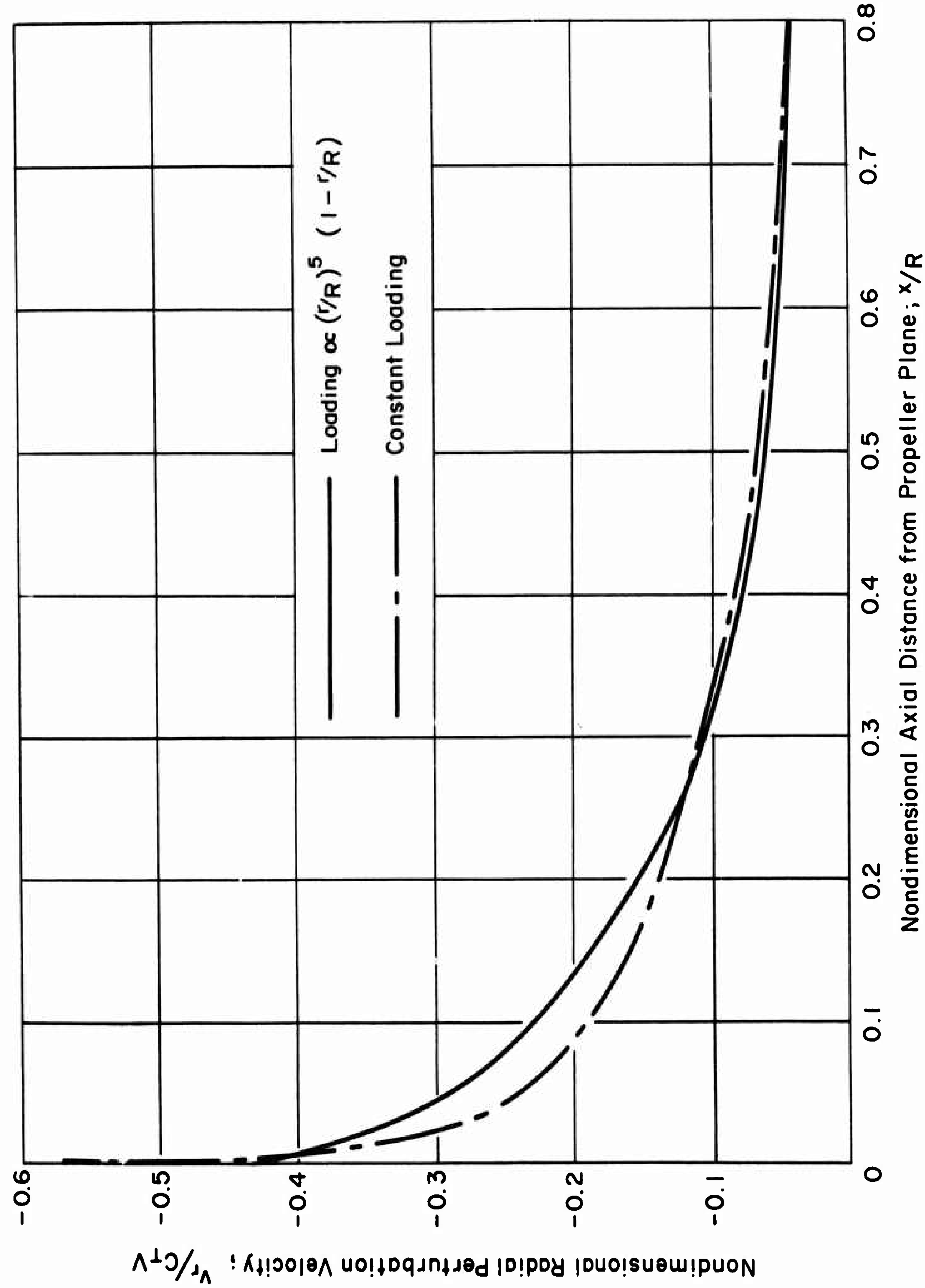

Figure 3 – Axial Variation of the Induced Radial Velocity at Propeller Radius

$$\frac{v_r(x,1)}{C_T V} = \frac{-1}{2\pi k_1} \left[\left(1 - \frac{k_1^2}{2}\right) K(k_1) - E(k_1) \right] \qquad [21]$$

in which E is the complete elliptic integral of the second kind, and

$$k_1^2 = \frac{4}{x^2+4} \qquad [22]$$

It is seen that as $x \to 0$, $v_r(x,1)$ behaves like ln x; it becomes singular at x = 0, as it is shown in Figure 3. This singular behavior may be expected for loadings which decrease to zero discontinuously at the propeller tip. This logarithmic singularity, as it is well known, is integrable. Therefore, the streamline is continuous at the propeller tip, but with an infinite slope. In reality, this singular behavior will not be present since the loading may decrease to zero quite sharply, but never discontinuously. Furthermore, the viscous nature of the fluid would prohibit the presence of infinite velocities. It is seen from Figure 3, that for $x/R > 0.3$, the values of $v_r(x,1)$ due to these two different loadings are quite similar.

III. Streamline Shape.

Along a streamline, the following relation holds:

$$\frac{dr}{dx} = \frac{v_r}{V+v_x} \quad . \qquad [23]$$

Consistent with the assumptions made to arrive at the linearized equation of motion, v_x may be neglected comparing with V. The streamline shape is then,

$$r-1 = \int_0^x \frac{v_r}{V} \, dx. \qquad [24]$$

Using the results obtained in the last section for the radially non-uniform loading, this above integration is performed numerically and the results are shown in Figure 4. In the uniformly loaded case, we expand both K and E in terms of $k_1' = \sqrt{1-k_1^2}$; then by termwise integration, we obtain

$$r - 1 = \frac{1}{2\pi} \left\{ \left[0.386 - \ln k_1' \right] k_1' + (0.04 - 0.75 \ln k_1')(k_1')^3 + \ldots \right\} \quad [25]$$

The results are also shown in Figure 4. It is seen that the maximum difference between these two results is about 0.01 $C_T R$. However, this may incur as much as 14 percent relative difference between the mean radial velocities calculated for these two different loadings. Both loadings lead, of course, to the same asymptotic value of r at distances far from the propeller.

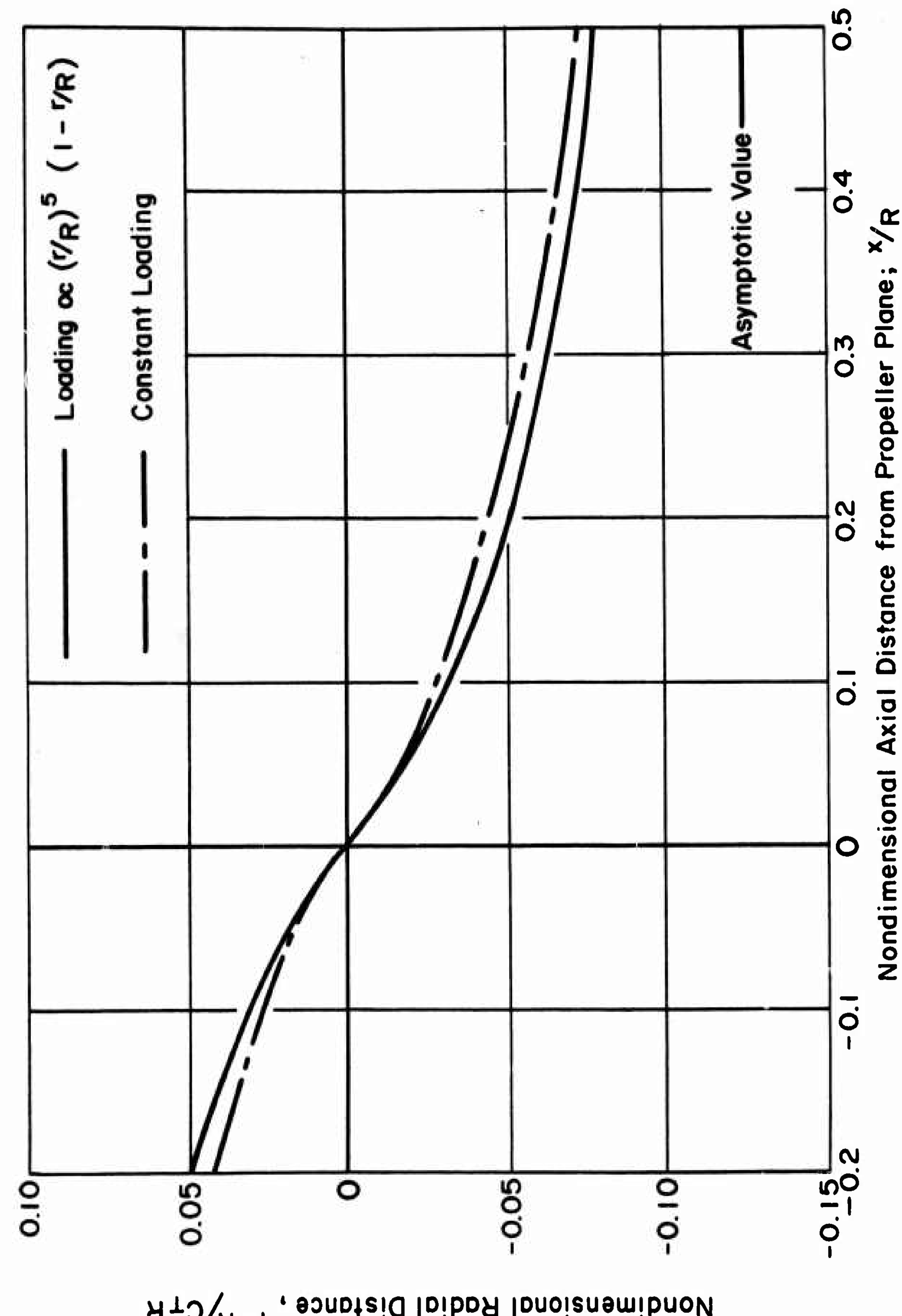

Figure 4 – Streamline Shape near the Periphery of the Propeller

REFERENCES

Jahnke, E., and Emde, F., (1945), Tables of Functions, Dover Publications, New York.

Kellogg, O. D., (1953), Foundations of Potential Theory, Dover Publications, New York.

Korvin-Kroukovsky, B. V., (1956), Stern Propeller Interaction with a Streamline Body of Revolution, International Shipbuilding Progress, Vol. 3, No.17.

Küchemann, D., and Weber, J., (1953), Aerodynamics of Propulsion, McGraw-Hill Book Co., Inc., New York.

Meyerhoff, L., and Finklestein, A. B., (1958), On Theories of the Duct Shape for a Ducted Propeller, PIBAL Report No. 484, Department of Aeronautical Engineering and Applied Mechanics, Polytechnic Institute of Brooklyn.

Tachmindji, A. J., (1959), The Axial Velocity Field of An Optimum Infinitely Bladed Propeller, David Taylor Model Basin Report No. 1294.

Tallqvist, H., (1938), Sechsstellige Tafeln der 32 erstern Kugelfunctionen P_n $(\cos\theta)$, Acta Societatis Scientiarum Fennicae, Nova Series A., Tom II, No. 11.